



**University of  
Zurich**<sup>UZH</sup>

**Zurich Open Repository and  
Archive**

University of Zurich  
University Library  
Strickhofstrasse 39  
CH-8057 Zurich  
[www.zora.uzh.ch](http://www.zora.uzh.ch)

---

Year: 2014

---

**Purification of fire derived markers for  $\mu\text{g}$  scale isotope analysis ( $\delta^{13}\text{C}$ ,  $\Delta^{14}\text{C}$ ) using  
high performance liquid chromatography (HPLC)**

Gierga, Merle ; Schneider, Maximilian P W ; Wiedemeier, Daniel B ; Lang, Susan Q ; Smittenberg, Rienk H ;  
Hajdas, Irka ; Bernasconi, Stefano M ; Schmidt, Michael W I

DOI: <https://doi.org/10.1016/j.orggeochem.2014.02.008>

Posted at the Zurich Open Repository and Archive, University of Zurich

ZORA URL: <https://doi.org/10.5167/uzh-100889>

Journal Article

Accepted Version

Originally published at:

Gierga, Merle; Schneider, Maximilian P W; Wiedemeier, Daniel B; Lang, Susan Q; Smittenberg, Rienk H; Hajdas, Irka; Bernasconi, Stefano M; Schmidt, Michael W I (2014). Purification of fire derived markers for  $\mu\text{g}$  scale isotope analysis ( $\delta^{13}\text{C}$ ,  $\Delta^{14}\text{C}$ ) using high performance liquid chromatography (HPLC). *Organic Geochemistry*, 70:1-9.

DOI: <https://doi.org/10.1016/j.orggeochem.2014.02.008>

1 Purification of fire-derived markers for  $\mu\text{g}$  scale isotope analysis ( $\delta^{13}\text{C}$ ,  
2  $\Delta^{14}\text{C}$ ) using high-performance liquid chromatography (HPLC)

3 Merle Gierga<sup>a\*</sup>, Maximilian P.W. Schneider<sup>b</sup>, Daniel B. Wiedemeier<sup>b</sup>, Susan Q. Lang<sup>a,1</sup>, Rienk H. Smittenberg<sup>c</sup>,  
4 Irka Hajdas<sup>d</sup>, Stefano M. Bernasconi<sup>a</sup>, Michael W.I. Schmidt<sup>b</sup>

5 <sup>a</sup> *Department of Earth Sciences, ETH Zürich, Sonneggstrasse 5, 8092 Zürich, Switzerland*

6 <sup>b</sup> *Department of Geography, University of Zürich, 8057 Zürich, Switzerland*

7 <sup>c</sup> *Geological Sciences, Stockholm University, 10691 Stockholm, Sweden*

8 <sup>d</sup> *Laboratory of Ion Beam Physics, ETH Zürich, 8093 Zürich, Switzerland*

9 \* Corresponding author. E-mail address: merle.gierga@erdw.ethz.ch

10 <sup>1</sup> Present address: Department of Earth and Ocean Sciences, University of South Carolina, Columbia, SC 29208,  
11 USA

12 ABSTRACT

13 Black carbon (BC) is the residue of incomplete biomass combustion. It is ubiquitous in nature  
14 and, due to its relative persistence, is an important factor in Earth's slow-cycling carbon pool.  
15 This resistant nature makes pure BC one of the most used materials for  $^{14}\text{C}$  dating to elucidate  
16 its formation date or residence time in the environment. However, most BC samples cannot  
17 be physically separated from their matrices, precluding accurate  $^{14}\text{C}$  values. Here we present a  
18 method for radiocarbon dating of the oxidation products of BC, benzene polycarboxylic acids,  
19 thereby circumventing interference from extraneous carbon. Individual compounds were  
20 isolated using high performance liquid chromatography (HPLC) and converted to  $\text{CO}_2$  via wet  
21 chemical oxidation for  $^{13}\text{C}$  and  $^{14}\text{C}$  isotope analysis. A detailed assessment was performed to  
22 identify and quantify sources of extraneous carbon contamination with two process standards  
23 of distinct isotopic signatures. The average blank was  $1.6 \pm 0.7 \mu\text{g C}$  and had an average  
24 radiocarbon content of  $0.90 \pm 0.50 \text{ F}^{14}\text{C}$ . We successfully analyzed the  $^{14}\text{C}$  content of  
25 individual benzene polycarboxylic acids with a sample size as small as 20-30  $\mu\text{g C}$  after  
26 correcting for the presence of the average blank. The combination of  $\delta^{13}\text{C}$  and  $\text{F}^{14}\text{C}$  analysis  
27 helps interpret the results and enables monitoring of extraneous carbon contribution in a fast  
28 and cost efficient way. Such a molecular approach to radiocarbon dating of BC residues  
29 enables the expansion of isotopic BC studies to samples that have either been too small or  
30 strongly affected by non-fire derived carbon.

31 **Keywords:** Compound-specific radiocarbon and isotope analyses; CSRA; benzene  
32 polycarboxylic acids; HPLC

## 33 **1. Introduction**

34 The solid residues of incomplete biomass combustion are generally summarized under the  
35 term black carbon (BC). It is ubiquitous in nature and can be found in the atmosphere,  
36 sediments, water and ice (Goldberg, 1985) and includes a continuum of combustion products  
37 ranging from slightly charred biomass to char and charcoal to highly condensed refractory  
38 soot (Hedges et al., 2000; Masiello, 2004). Fire derived components are of interest for the  
39 investigation of the global C cycle due to their relative persistence in the environment. It is  
40 widely accepted that BC contributes significantly to the Earth's slow-cycling C pool  
41 (Skjemstad et al., 1996, 2001; Schmidt et al., 2000; Preston and Schmidt, 2006; Knicker et al.,  
42 2008) and in models of soil organic matter (OM) turnover it is defined as a C pool with  
43 relatively high resistance to degradation (Skjemstad et al., 2004). It is also utilized in the  
44 reconstruction of fire history from geological records (e.g. Glaser et al., 2000; Carcaillet et al.,  
45 2002; Tinner et al., 2005). Similarly, pure charcoal is of importance for archeological  
46 research; in addition, the presence of BC at excavation sites allows precise determination of  
47 the age of the finds from  $^{14}\text{C}$  analysis. Consequently, pieces of pure charcoal are one of the  
48 most targeted materials for  $^{14}\text{C}$  dating in archaeological or geological research (Bird et al.,  
49 1999).

50 Nevertheless, the physicochemical properties and the biological stability of BC are poorly  
51 understood and even quantification is inherently difficult. One promising approach towards a  
52 better understanding and quantification of BC is a molecular method, the so-called 'BPCA  
53 method' introduced by Glaser et al. (1998). Benzene polycarboxylic acids (BPCAs) result  
54 from the digestion of BC with  $\text{HNO}_3$  under high pressure and temperature, and can be  
55 analyzed using either gas chromatography (GC; Glaser et al., 1998) or high performance  
56 liquid chromatography (HPLC; Dittmar, 2008; Wiedemeier et al., 2013). The BPCAs derive  
57 unambiguously from BC and provide insight into the original BC at a molecular scale. In  
58 addition to being a quantifiable molecular proxy for the total amount of BC in a complex  
59 matrix, the relative distribution of individual BPCAs can provide further information. For  
60 example, a relatively high amount of highly carboxylated BPCAs such as mellitic acid  
61 (B6CA) and benzene pentacarboxylic acid (B5CA) is indicative of a high degree of  
62 condensation (Dittmar, 2008; Schneider et al., 2011). The numbers in the notation indicate the  
63 number of substituted carboxylic acid groups per benzene ring.

64 The radiocarbon signature of BPCAs has potential for elucidating the fate and source of BC in  
65 nature, as the concentration of  $^{14}\text{C}$  in a BC sample can be directly related to its age or mean  
66 residence time. For recent BC samples,  $^{14}\text{C}$  analysis allows source apportioning of the BC  
67 between fossil fuel derived charcoal that is depleted in  $^{14}\text{C}$  ( $\text{F}^{14}\text{C} 0$ ) and burned modern

68 biomass that reflects atmospheric radiocarbon content ( $F^{14}\text{C} \geq 1$ ). On the whole, there is an  
69 essential advantage in determining the  $^{14}\text{C}$  content of these specific biomarkers vs. dating of  
70 bulk BC samples (e.g. Ziolkowski and Druffel, 2009; Zimmerman, 2010; Yarnes et al., 2011).  
71 In particular, analysis of bulk samples frequently suffers from large uncertainty due to small  
72 sample size and the challenge in physically separating pure BC from interfering OM. For  
73 example, OM in soils and sediments is a complex mixture of compounds, which can range  
74 from recently produced compounds to very old material (Hedges et al., 2000). The same is  
75 true for buried archaeological samples. The matrix of pottery can contain organic carbon-  
76 bearing clay closely associated with the charred residue, or organic carbon can be taken up  
77 from the burial environment, causing further interference.

78 Eglinton et al. (1996) introduced the concept of compound-specific radiocarbon analysis  
79 (CSRA) applied to certain solvent extractable lipids. The first application using the BPCA  
80 method to date BC on a molecular scale was by Ziolkowski and Druffel (2009a), who  
81 separated individual BPCAs using preparative GC, and achieved reliable results with  
82 reasonably low and constant blanks. Nevertheless, the method has several drawbacks. BPCAs  
83 must be treated to form GC-amenable derivatives, requiring the addition of external C. The  
84 authors applied trimethylsilyl-diazomethane as derivatization agent. Even though it has been  
85 reported to be more efficient than other derivatization protocols (Ziolkowski and Druffel,  
86 2009b), it is known that losses can occur. This is also true for the most common derivatization  
87 technique, silylation with BSTFA (Schneider et al., 2011). Finally, a GC column has limited  
88 capacity, necessitating a number of injections to collect sufficient material for dating. Many  
89 of the problems can be circumvented by separating the BPCAs using HPLC (Dittmar, 2008;  
90 Wiedemeier et al., 2013).

91 In general,  $^{14}\text{C}$  analysis is sensitive to any contribution from extraneous carbon ( $C_{ex}$ ) added to  
92 the sample during the laboratory protocol. This is particularly true for ultra small scale  
93 samples containing  $< 30 \mu\text{g C}$ . Purification procedures for CSRA must therefore be designed  
94 to minimize and accurately quantify  $C_{ex}$  addition (Pearson et al., 1998; Shah and Pearson,  
95 2007; Ziolkowski and Druffel, 2009a; Birkholz et al., 2013; Lang et al., 2013).

96 In this study we present a new approach for molecular scale  $^{14}\text{C}$  analysis of fire-derived  
97 compounds on the basis of the separation of BPCAs using liquid chromatography  
98 (Wiedemeier et al., 2013) combined with a recent method of wet oxidation suitable for  
99 combined  $^{13}\text{C}$  and  $^{14}\text{C}$  isotope analysis (Lang et al., 2012, 2013). The method allows sample  
100 oxidation despite the presence of concentrated  $\text{H}_3\text{PO}_4$ , which is essential for achieving  
101 separation of the BPCAs with HPLC. The direct conversion of the BPCAs to  $\text{CO}_2$  within a gas  
102 tight vial allows the sample gas to be subsampled for  $\delta^{13}\text{C}$  analysis prior to injection for  
103 accelerator mass spectrometry (AMS).

104 We describe the successful purification of individual B5CAs and B6CAs followed by  $\delta^{13}\text{C}$   
105 and  $\text{F}^{14}\text{C}$  analysis. A detailed blank assessment was carried out using direct and indirect  
106 approaches to assess the amount and the isotopic signature of  $C_{\text{ex}}$ . Two different types of  
107 charcoal were selected as standards. The first was an archaeological charcoal with a  $^{14}\text{C}$  age >  
108 50000 BP ( $\leq 0.02 \text{ F}^{14}\text{C}$ ) and the second a modern charcoal ( $\geq 1 \text{ F}^{14}\text{C}$ ) prepared from a  
109 recently cut tree. Together they represented the end members of  $^{14}\text{C}$  analysis and thereby  
110 allowed a good evaluation of this new method for BC dating.

## 111 **2. Experimental**

112 The data were produced from two successive series of experiments. Both included HPLC  
113 isolation followed by wet oxidation, GC-isotope ratio mass spectrometry (GC-IRMS) and  
114 AMS measurements. All glassware was pre-heated to 450 °C for 5 h prior to use to remove  
115 organic contaminants. Ultra pure water was supplied from a MilliQ Advantage A10 system  
116 (Millipore, USA) and all chemicals were of the highest available grade and were tested for  
117 impurities before use.

### 118 *2.1. Process standards*

119 The archaeological charcoal sample ('fossil char') was from in situ charred trees sampled  
120 from paroxysmal flow deposits in the Maninjau caldera in West-Central Sumatra (Alloway et  
121 al., 2004). Its precise dating using conventional AMS demonstrated that it lacked  $^{14}\text{C}$  and had  
122 an age of ca. 50 ka BP (Alloway et al., 2004; Ascough et al., 2009). The modern analog  
123 ('modern char') was produced from chestnut wood (*Castanea sativa*) from a single tree cut in  
124 a forest in Southern Switzerland. The wood was charred at 450 °C for 5 h under a  $\text{N}_2$   
125 atmosphere (Hammes et al., 2006).

126 The samples were of almost pure charcoal, one was recovered in-situ and the other was  
127 produced in the laboratory under controlled conditions, allowing the assumption that they  
128 were not significantly affected by interfering C-bearing material. Therefore the radiocarbon  
129 contents of the bulk samples were expected to be the same as that of the isolated BPCAs.  
130 Bulk subsamples were analyzed for  $^{14}\text{C}$  content as solid targets at the Laboratory of Ion Beam  
131 Physics of the ETH Zürich, Switzerland after being sequentially extracted with acid and base  
132 reagents to remove contaminants from the surfaces. The so-called acid-base-acid (ABA)  
133 treatment is a standard cleaning procedure prior to  $^{14}\text{C}$  analysis (Hajdas et al., 2004). The  $^{14}\text{C}$   
134 content of the fossil char was found to be  $0.003 \pm 0.001 \text{ F}^{14}\text{C}$  (ETH-50456). The modern char  
135 was produced from unaltered dried wood that had a  $^{14}\text{C}$  content of  $1.142 \pm 0.004 \text{ F}^{14}\text{C}$  (ETH-  
136 50458) and its charred residue was almost identical at  $1.149 \pm 0.004 \text{ F}^{14}\text{C}$  (ETH-50457).  
137 These values were used as reference values.

138 *2.2. Sample extraction and purification*

139 Extraction and purification of BPCAs was carried out according to the protocol of  
140 Wiedemeier et al. (2013) with modifications to make it amenable for CSRA. In brief, 15-25  
141 mg of the dried and milled sample was directly digested in a quartz tube with 2 ml HNO<sub>3</sub> (65  
142 wt.% or 14.4 mol/l) at 170 °C for 8 h. After cooling, the aqueous solution was filtered over  
143 pre-rinsed quartz fiber filters. The extract was eluted over a cation exchange resin and freeze  
144 dried to remove water and acid. The dried residue was dissolved in MeOH/water (1:1, v/v)  
145 and applied to a pre-conditioned C<sub>18</sub> solid phase extraction cartridge to remove apolar  
146 components. Finally, the eluate was dried again using an Eppendorf concentrator system.

147 *2.3. HPLC purification*

148 Individual BPCAs were isolated using an Agilent 1290 Infinity UPLC instrument (Santa  
149 Clara, USA). Separation was achieved with an Agilent Poroshell 120-SB C<sub>18</sub> column (4.6 ×  
150 100 mm, 2.7 μm pore size) using a gradient of diluted ortho H<sub>3</sub>PO<sub>4</sub> buffered to pH 1.2 with  
151 NaH<sub>2</sub>PO<sub>4</sub> (mobile phase A) and pure MeCN (mobile phase B). Compounds were detected  
152 with an Agilent 1290 Infinity diode array detector at 216 and 240 nm.

153 Extracted samples ('total digest') were diluted in ultra pure water to achieve a concentration  
154 of B5CA and B6CA of ca. 200 ± 50 ng C/ μl for HPLC injection. A small (1 μl) initial  
155 injection was made to quantify the peaks and assign retention times. Larger (5 μl) injections  
156 (10-30 in total) were then made for fraction collection. The mobile phase was collected during  
157 the time windows corresponding to the elution of the B5CA and B6CA compounds into pre-  
158 combusted glass vials with a time-programmed analytical fraction collector (Agilent 1260  
159 AS-FC). The collected fractions were transferred to screw cap vials with borosilicate pipettes  
160 and dried under a stream of N<sub>2</sub> to remove all mobile phases with the exception of non-volatile  
161 H<sub>3</sub>PO<sub>4</sub>. Before drying, a small aliquot was re-injected on HPLC to assess the recovery and  
162 purity of the isolated compounds. Quantification was carried out with an external standard  
163 series that contained a mixture of commercially available BPCAs (Wiedemeier et al., 2013).

164 *2.4. Wet oxidation*

165 The compound-specific isotopic signature (δ<sup>13</sup>C, F<sup>14</sup>C) of isolated BPCAs was determined  
166 with the methods described by Lang et al. (2012, 2013). Specifically, isolated and acidified  
167 samples were transferred to 12 ml gas tight vials, diluted with Milli-Q water to a total volume  
168 of 4 ml, and spiked with 0.75 ml supersaturated oxidizing solution (100 ml H<sub>2</sub>O + 2.0 g  
169 K<sub>2</sub>S<sub>2</sub>O<sub>8</sub> + 200 μl 85% H<sub>3</sub>PO<sub>4</sub>). Vials were sealed using a standard cap with a butyl rubber  
170 septum and flushed with high purity He (grade 5.0, 99.999%) for 8 min at 125 ml/min to  
171 remove atmospheric CO<sub>2</sub> from the headspace. The output gas stream passed through a water

172 trap to prevent backflow of atmospheric CO<sub>2</sub>. Then, the vials were heated to 100 °C for 60  
173 min to oxidize the BPCAs to CO<sub>2</sub>. Samples were allowed to cool to room temperature  
174 overnight. Modern sucrose [Sigma Aldrich, P/N S7903, lot 090M02112V, F<sup>14</sup>C 1.053 ± 0.03  
175 (ETH-47293)] and <sup>14</sup>C-free phthalic acid [Sigma Aldrich, P/N 80010, lot 1431342V, F<sup>14</sup>C ≤  
176 0.0025 (ETH-42443)] were used to assess the addition of external carbonaceous material  
177 during oxidation and transfer. Both were oxidized and analyzed for δ<sup>13</sup>C and F<sup>14</sup>C.

#### 178 2.5. Stable carbon isotope analysis (δ<sup>13</sup>C)

179 The stable carbon isotopic composition of the headspace CO<sub>2</sub> was measured with two  
180 approaches. For initial tests, we analyzed the C content of various blank samples to determine  
181 background values, while the isotopic composition was of secondary interest. These samples  
182 were analyzed on a GasBench II on-line gas preparation and introduction system (Thermo  
183 Fisher Scientific, Bremen, Germany) coupled to a ConFlo IV interface and a Delta V Plus  
184 mass spectrometer (both Thermo Fisher Scientific), allowing the accurate detection of C  
185 content and <sup>13</sup>C of samples as small as 5 µg C. As δ<sup>13</sup>C analysis with the GasBench uses the  
186 majority of the CO<sub>2</sub>, samples were also analyzed with a second method designed to preserve  
187 the majority of the CO<sub>2</sub> for <sup>14</sup>C analysis. In this approach, 100 µl of headspace gas was  
188 removed from the vials with a gastight syringe (Hamilton). The gas was injected into a gas  
189 chromatograph (Agilent 6890) with a split/splitless inlet and which was directly connected to  
190 a Delta V Plus via a ConFlo IV interface (both Thermo Fisher Scientific, Bremen, German).  
191 CO<sub>2</sub> was separated from interfering gases with a CP Poraplot Q column (27.5 m × 0.32 µm;  
192 10 µm; Varian) maintained at 100 °C and a He flow rate of 2.0 ml/min.

193 The raw δ<sup>13</sup>C values of each series of samples were corrected for fractionation effects  
194 between headspace and dissolved CO<sub>2</sub>, as well for blank values and instrumental drift using  
195 standards of known composition (Lang et al., 2012). The amount of C was calculated by  
196 comparison with a dilution series of phthalic acid.

#### 197 2.6. Radiocarbon analysis (F<sup>14</sup>C)

198 Radiocarbon analysis was carried out at the Laboratory for Ion Beam Physics of ETH Zürich,  
199 Switzerland using the MICADAS (mini carbon dating system) equipped with a gas ion source  
200 (Ruff et al., 2007; Synal et al., 2007) that allows direct introduction of CO<sub>2</sub> from the  
201 headspace into the gas ion source. Detailed descriptions about the instrumentation can be  
202 found elsewhere (Lang et al., 2013; Wacker et al., 2013). In brief, sample CO<sub>2</sub> was removed  
203 from the vials by flushing with He and diverting the output over a magnesium perchlorate  
204 water trap to a trap containing X13 zeolite molecular sieve, which adsorbs CO<sub>2</sub> at room  
205 temperature. After trapping, a valve was toggled to connect the trap to a gas tight syringe, and

206 the CO<sub>2</sub> was released by heating the zeolite to 450 °C. The amount of CO<sub>2</sub> in the syringe was  
207 detected pneumatically to allow dilution of the sample gas with He to 5 %, v/v CO<sub>2</sub> in He.  
208 This gas mixture was then pushed continuously out of the syringe into the ion source. Oxalic  
209 acid I (OX-1) gas was used as a modern standard (Stuiver and Polach, 1977) for  
210 normalization and fossil CO<sub>2</sub> gas served as a blank.

211 The raw data output was processed with the BATS software (Wacker et al., 2010) so that the  
212 results are reported as fraction modern (F<sup>14</sup>C; Reimer et al., 2004) being corrected for  
213 instrumental background, standard normalization and evaluated for uncertainty. Further  
214 corrections for wet oxidation and purification of BPCAs are discussed below.

### 215 **3. Results and Discussion**

#### 216 *3.1. Isolation of individual BPCAs with HPLC*

217 The first goal in method development was the definition of appropriate chromatographic  
218 conditions for providing sufficient amounts of the pure target compounds. BPCA  
219 concentrations in the total digests were determined following Wiedemeier et al. (2013). In  
220 both samples B6CA and B5CA represented ca. 80 % of the total quantified BPCA-C. For  
221 CSRA these two compounds provided the best conditions for successfully isolating and  
222 dating them. As a second step we injected as much as 1 µg C from each of the two target  
223 compounds and were still able to define robust retention times of the baseline separated  
224 peaks. Even though the column was slightly overloaded, no tailing of the target peaks to other  
225 fractions was observed (Fig. 1A) by re-injection of the eluent collected just before and after  
226 collection of the sample peak. The time window for fraction collection was set as narrow as  
227 possible to minimize the amount of potential co-eluting extraneous compounds and,  
228 especially, column bleed. Next to the quantified BPCAs a suite of other peaks are present (Fig  
229 1A). These were other by-products of the digestion and were most likely nitrated BPCAs  
230 (Ziolkowski and Druffel, 2009b). We isolated B5CA and B6CA fractions from both process  
231 standards, the fossil and modern char, in 3 replicates, respectively. As a preliminary  
232 assessment of  $C_{ex}$ , aliquots of the collected fractions were re-injected; this did not show any  
233 UV-detectable contaminants (Fig. 1B). Fractions were typically collected and combined from  
234 20 to 30 repeated injections. Sample recovery varied between 50 and 84% (Table 1). Losses  
235 might have occurred during fraction collection or during transfer and concentration of the  
236 individual fractions. We did not detect significant amounts of the target compounds in  
237 fractions collected subsequently after the time window for B6CA or B5CA, which suggests  
238 that no significant tailing occurred after passing the detector and before the fraction collector.  
239 As we considered it more important to avoid the collection of other peaks eluting shortly after



240 the target compounds, we did not try to optimize the recovery widening the collection  
241 window, as soon as recovery exceeded 50%. Isotopic fractionation effects over the  
242 chromatographic peak were not expected for the  $^{14}\text{C}$  content (Zencak et al., 2007). This can be  
243 explained by the fact that  $F^{14}\text{C}$  values are corrected for isotopic fractionation, which is  
244 expected to occur during AMS analysis. It is also possible that losses occurred during the  
245 transfer and concentration of the collected sample volumes. Up to 15 ml of that aqueous  
246 solution had to be reduced to a final volume of 2 ml, resulting in a high concentration of  
247  $\text{H}_3\text{PO}_4$  as only water and MeCN were volatilized under  $\text{N}_2$  flow.

### 248 3.2. Wet oxidation and $\delta^{13}\text{C}$ values

249 The wet oxidation method was originally designed to oxidize organic acids (Lang et al. 2012;  
250 2013) but proved to be also suitable for BPCAs. The oxidation efficiency was tested by  
251 oxidizing a known amount of a benzene pentacarboxylic acid standard, with recovery always  
252  $> 90\%$ . Furthermore, no isotopic fractionation was observed when the  $\delta^{13}\text{C}$  values of the  
253 oxidized standard material were compared with the reference values obtained with total  
254 combustion of the bulk sample powder using elemental analysis (EA)-IRMS. Attempts to  
255 further optimize the oxidation parameters by varying temperature and reaction time did not  
256 result in improvement of recovery. Wet oxidation of a mellitic acid standard gave consistent  
257 results compared with the B5CA standard.

258 The final  $\delta^{13}\text{C}$  values of each isolated B5CA or B6CA sample, as well of the entire digestion  
259 extracts are listed in Table 1. The values are corrected for fractionation effects between the  
260 liquid and gas phase and for process and instrumental background of the wet oxidation  
261 procedure itself, as described by Lang et al. (2012). In brief, the process blank was  
262 determined using oxidized ultra pure water with similar volumes to the samples. The peak  
263 area of these blanks averaged  $0.55 \pm 0.09 \text{ V}\cdot\text{s}$  ( $n = 3$ ), which corresponds to a value near the  
264 limit of detection of  $\leq 0.2 \mu\text{g C}$ . As these peaks were too small for reliable  $\delta^{13}\text{C}$  values, the  
265 isotopic composition of the process blank was estimated indirectly by comparing the values  
266 for the oxidized phthalic acid standard samples with the known reference value. The  $\delta^{13}\text{C}$  of  
267 the blanks is very sensitive, so it was individually calculated for each prepared series. The  
268 blanks were calculated to be  $-14.1 \pm 1.1\text{‰}$  for the first and  $-9.1 \pm 1.1\text{‰}$  for the second series.  
269 At first sight, there is a significant difference between the two blanks. It should be taken into  
270 account, however, that small differences detected with such small signals could lead to large  
271 differences in the  $\delta^{13}\text{C}$  values for the blanks. The isotopic shift of ca.  $5\text{‰}$  for the blank results  
272 probably resulted from slightly changes in the quality of the chemicals in use, for instance the  
273 oxidizing reagent or the ultra pure water. This assumption is supported by the fact that the  
274  $\delta^{13}\text{C}$  values for the fire-derived compounds from the fossil and modern char showed no

275 significant difference after being corrected for the blank value for the wet oxidation procedure  
276 (Table 1). The BPCAs had slightly lower  $\delta^{13}\text{C}$  values than the total digests (Fig. 2), while  
277 B5CA was more negative than B6CA. These small differences may be the result of  
278 inhomogeneity of the parent material. Another explanation might be an incomplete collection  
279 of the chromatographic peak, as  $\delta^{13}\text{C}$  values are much more sensitive to fractionation effects  
280 than  $F^{14}\text{C}$  values (Zencak et al., 2007). The overall reproducibility ( $1\sigma$ ) was  $\leq 0.7\%$ . Even if  
281 this is slightly higher than the reported precision for the chemical oxidation method ( $\leq 0.4\%$ ,  
282 Lang et al., 2012), the values are still satisfyingly accurate. With this technique, only a very  
283 small part of the isolated samples was used for stable isotope analysis in order to assure large  
284 enough samples for the AMS analysis. More accurate results could potentially be achieved by  
285 isolating a separate sample dedicated only to  $\delta^{13}\text{C}$  using a GasBench device.

286 For the modern charcoal, we compared the isotopic composition of total digests and  
287 compound-specific  $\delta^{13}\text{C}$  values with data from Yarnes et al. (2011), who successfully  
288 performed continuous flow  $^{13}\text{C}$  analysis after separation of BPCAs using a laborious 2 h ion  
289 exchange chromatography method. The values of Yarnes et al. (2011) are shown in Fig. 2 for  
290 direct comparison with our results. Their results for B5CA and B6CA from the modern char  
291 were within the error of our results. Furthermore, we obtained values for the BPCA extract of  
292 the modern char comparable to their value obtained using EA-IRMS analysis with the bulk  
293 sample. Compared with our distinct results the reported values by Yarnes et al. (2011) were  
294 systematically shifted by a value as small as  $-0.5\%$ , which is still in the range of the precision  
295 of both studies. This comparison demonstrates that our method for analyzing the  $\delta^{13}\text{C}$  values  
296 of BPCAs is of high quality and can be performed on a very small aliquot of a sample whose  
297 main part is needed for CSRA.

### 298 3.3. Assessment of extraneous carbon

299 As mentioned above, radiocarbon analysis is more sensitive to the addition of extraneous C  
300 than  $\delta^{13}\text{C}$  analysis (e.g. Shah and Pearson, 2007; Ziolkowski and Druffel, 2009a). It is  
301 therefore mandatory to minimize and precisely determine the contribution from  $C_{ex}$  to carry  
302 out an appropriate blank correction and obtain reliable radiocarbon values. Generally  
303 speaking, a measured  $F^{14}\text{C}$  value is composed of a contribution from both the compound of  
304 interest and from  $C_{ex}$ . This can be expressed with the following mass balance equation:

$$305 \quad F_T \cdot C_T = F_S \cdot C_S + F_{ex} \cdot C_{ex} \quad (1)$$

306 Where  $F$  is the  $F^{14}\text{C}$  value and  $C$  the amount of carbon in  $\mu\text{g}$ . The subscript  $T$  refers to total as  
307 measured,  $S$  to sample and  $ex$  to extraneous. In order to solve the equation for  $F_S$ , the amount  
308 and radiocarbon content of  $C_{ex}$  need to be determined beforehand, given that  $C_S = C_T - C_{ex}$ .

309 There are several possible sources of contaminating C added to the sample. Considering the  
310 entire laboratory protocol, it might be taken up during the extraction and cleaning procedure  
311 ( $C_{chemistry}$ ), the HPLC isolation ( $C_{HPLC}$ ), the wet oxidation procedure ( $C_{ox}$ ) and finally during  
312 the AMS analysis itself ( $C_{AMS}$ ). Accordingly  $C_{ex}$  can be expressed as a sum of the following  
313 components:  $C_{ex} = C_{chemistry} + C_{HPLC} + C_{ox} + C_{AMS}$ . The most straightforward way to trace back  
314 to  $C_{ex}$  is to start at the end of the laboratory protocol, going back to the first steps.

### 315 3.3.1. $C_{AMS}$

316 The AMS instrumental background is routinely determined during each measurement  
317 campaign. As mentioned above, reported values are normalized using the results of small  
318 scale Ox-I standards and are corrected for small scale AMS blanks using the BATS software  
319 (Wacker et al., 2010). Because of this,  $C_{AMS}$  is not discussed further here. Accordingly, the  
320 subscript  $T$  ( $F^{14}C_T$ ,  $C_T$ ) indicates in the following that the raw values had already been  
321 corrected with the BATS software.

### 322 3.3.2. $C_{ox}$

323 The contribution of  $C_{ex}$  added during wet oxidation was calculated indirectly using two  
324 standards of known radiocarbon content ( $^{14}C$ -free phthalic acid and modern sucrose). With  
325 this method it is possible to assess separately two contaminant fractions. A detailed  
326 description of the method is given by Lang et al. (2013). As we adopted the approach for the  
327 assessment of  $C_{chemistry}$  and  $C_{HPLC}$ , further information is given in the following section.

328 For the samples measured during the first campaign, we determined a small influence from a  
329 modern  $C_{ox}$  source, corresponding to  $0.13 \pm 0.04 \mu\text{g C}$  ( $n = 5$ ), whereas the contribution from  
330 radiocarbon-dead  $C_{ox}$  corresponded to  $0.85 \pm 0.44 \mu\text{g C}$  ( $n = 5$ ). In combination, this resulted  
331 in a total blank of  $0.97 \pm 0.44 \mu\text{g C}$  with a  $F^{14}C$  value of  $0.13 \pm 0.07$ . For the second  
332 measurement campaign, we were able to reduce the amount of  $C_{ox}$  via  $0.07 \pm 0.03 \mu\text{g C}$   
333 modern  $C_{ox}$  and  $0.45 \pm 0.43 \mu\text{g C}$  of radiocarbon-dead material, i.e. a total of  $0.52 \pm 0.44 \mu\text{g C}$   
334  $C_{ox}$  with  $0.14 \pm 0.13 F^{14}C$ . Evaluation of the first data set pointed to some sources of  $C_{ox}$  that  
335 could easily be reduced, especially for the reagent used for the wet oxidation. The reagent was  
336 recrystallized 2x in water before use during the second campaign. This resulted in a reduction  
337 of radiocarbon-dead  $C_{ox}$  of ca.  $0.5 \mu\text{g C}$  per sample, while the average  $F^{14}C$  of  $C_{ox}$  remained  
338 comparable with the  $F_{ox}$  determined for the first campaign. The correction for  $C_{ox}$  was applied  
339 to all samples before determining  $C_{chemistry}$  and  $C_{HPLC}$ . The corrected values are indicated as  
340  $C_T$  and  $F^{14}C_T$  in the following.

### 341 3.3.3. $C_{chemistry}$ and $C_{HPLC}$

342 Initially, we directly collected and analyzed  $C_{chemistry}$  and  $C_{HPLC}$ . Blank samples were run  
343 through the entire laboratory protocol except for radiocarbon dating. Another set of blanks  
344 was produced, performing only the HPLC step, omitting the extraction procedure. Because  
345 the total amount of extraneous C was very low, the number of injections and the duration of  
346 the fraction collection window were increased vs. regular sample fraction collection. The  
347 amount of C and its  $\delta^{13}C$  values were determined by analyzing all material with the GasBench  
348 device (Table 2), which gives better accuracy than the GC option described above. For one  
349 sample, it was not possible to obtain a reliable  $\delta^{13}C$  value, as the sample size was too small.  
350 The average blank that passed both extraction and HPLC contained  $0.23 \pm 0.12 \mu\text{g}$   
351  $C_{chemistry+HPLC} \text{ ml}^{-1}$  ( $n = 2$ ), whereas  $C_{HPLC}$  showed an average of  $0.22 \pm 0.04 \mu\text{g ml}^{-1}$  ( $n = 5$ ).  
352 This showed that the chemical extraction process ( $C_{chemistry}$ ) did not significantly contribute to  
353 the amount of the sum of  $C_{ex}$  and could be assumed to be zero. Most likely, if any  $C_{chemistry}$   
354 were present, it would again be removed during the HPLC purification step to a level below  
355 the detection limit. The isotopic signatures of the  $C_{HPLC}$  replicates showed comparable values,  
356 within a relatively larger error due to the small sample sizes. The  $\delta^{13}C$  value of  $C_{HPLC}$   
357 averaged  $-29.5 \pm 1.3\text{‰}$  (Table 2), implying that the source of  $C_{ex}$  remained constant and that  
358 no unexpected and uncontrolled addition of  $C_{ex}$  occurred. Separate analysis of the aqueous  
359 eluent before usage showed that this was most probably the main source of  $C_{HPLC}$ , as it  
360 already contained  $0.3 \pm 0.1 \mu\text{g C/ml}$ . Future efforts to reduce  $C_{HPLC}$  should therefore focus on  
361 the mobile phase in the HPLC step.

362 A strong relationship ( $R^2 0.91$ ) existed between the collected volumes of  $C_{HPLC}$  and their C  
363 content (Fig. 3). The intercept of near zero suggests that any constant background was absent,  
364 while the slope ( $0.22 \mu\text{g C ml}^{-1}$ ) of the linear regression represented the amount of  $C_{HPLC}$   
365 eluting per ml eluent. Therefore, multiplying this value by the volume collected for a specific  
366 sample should give a preliminary estimate of  $C_{HPLC}$  for an individual sample, enabling  
367 calculation of  $F_{HPLC}$  for each sample. However, we discovered that this estimate was not  
368 accurate enough: calculated values of  $C_{HPLC}$  for individual samples ranged between 0.9 and  
369  $2.1 \mu\text{g C}$ , resulting in reasonable estimates for  $F_{HPLC}$  for some samples (Supplementary  
370 material), but also in non-natural values of  $F_{HPLC} > 2$  for others. Interestingly, the averaged  
371 values for  $F_{HPLC}$  for each process standard were at the same level of a blank with a modern  
372 radiocarbon value ( $F^{14}C \approx 1$ ).

373 It is also possible to determine the blank contribution ( $C_{HPLC}$ ) and its radiocarbon signature  
374 ( $F_{HPLC}$ ) indirectly. For this approach,  $C_{ex}$  needs to be assumed as a constant amount of carbon  
375 being added to each sample during sample preparation. It is based on the theoretical  
376 assumption that the  $F_{ex}$  would be composed of two pools characterized by opposite  $^{14}C$   
377 content (i.e. modern and  $^{14}C$ -free). The combination of the results from two standards with

378 that with opposite  $^{14}\text{C}$  content then allows a mathematical solution for both unknowns, here  
379  $C_{HPLC}$  and  $F_{HPLC}$ . It is a common approach to determine a theoretical contribution from  
380 modern  $C_{ex}$  ( $F^{14}\text{C} = 1$ ) by use of a radiocarbon-dead ( $F^{14}\text{C} = 0$ ) process standard and vice  
381 versa (Shah and Pearson, 2007; Ziolkowski and Druffel, 2009a; Lang et al., 2013). For this,  
382 Eq. 1 was re-arranged and modified:

$$383 \quad C_{HPLC} = (F_T \cdot C_T - F_S \cdot C_S) / (F_{HPLC} - F_S) \quad (2)$$

384 Accordingly, a  $C_{HPLC}$  value for each replicate of fossil char was calculated assuming  $F_{HPLC} = 1$   
385 and similarly for the modern char, assuming  $F_{HPLC} = 0$  (Table 3). To solve the equation the  
386 reference values from the bulk powder were used as  $F_S$ . The average modern  $C_{HPLC}$  based on  
387 the individual B5CAs and B6CAs from the fossil charcoal, was  $1.4 \pm 0.5 \mu\text{g C}$  ( $n = 5$ ; Table  
388 3). In contrast, the BPCAs isolated from the modern char sample were hardly affected (Fig.  
389 3), resulting in an average contribution of  $^{14}\text{C}$ -free  $C_{HPLC}$  of  $0.2 \pm 0.4 \mu\text{g C}$ .

390 While the subdivision of the amount of blank C into two pools is a convenient mathematical  
391 concept, in nature it is more likely that there is a single C pool with a distinct  $^{14}\text{C}$  signature  
392 displaying a mean value of all various compounds. In order to determine more realistic  
393 values,  $C_{ex}$  and  $F_{ex}$  can be combined by addition of the two theoretical  $C_{ex}$  values and by  
394 calculating the weighted average of the two  $F_{ex}$  values:

$$395 \quad F_{ex} = (F_{modern} \cdot C_{modern} + F_{dead} \cdot C_{dead}) / (C_{modern} + C_{dead}) \quad (3)$$

396 While the subscript  $ex$  can be substituted with the subscript describing the respective part of  
397 the sample preparation. Here, it resulted in  $C_{HPLC} = 1.6 \pm 0.7 \mu\text{g C}$  with an average  
398 radiocarbon content  $F_{HPLC}$  of  $0.90 \pm 0.50 F^{14}\text{C}$ . This amount was satisfyingly low for samples  
399 with  $> 15 \mu\text{g C}$ . Consequently, a fossil source for  $C_{HPLC}$  can be excluded; nevertheless, it is  
400 hardly possible to directly identify the origin of  $C_{HPLC}$ . A significant change of  $F_{HPLC}$  during  
401 later measurements is though a clear indication for additional contribution of  $C_{HPLC}$ , in  
402 general.

403 Fig. 3 illustrates the size-dependent relationship of the radiocarbon content of the samples not  
404 corrected for  $C_{HPLC}$  vs. the theoretically modeled  $F_{HPLC}$  deduced from the mixture of a  $C_S$  with  
405 varying sample size and the constant  $C_{HPLC}$ . Note that the given data set does not show a  
406 significant dependence between the amounts of repeated injections (i.e. the amount of  
407 collected mobile phase) and  $C_{HPLC}$ . However, the opposite was concluded after direct analysis  
408 of  $C_{HPLC}$  (Fig. 3). This apparent contradiction can be attributed to the fact that the process  
409 samples were only collected over 20 to 30 injections, with a total of 4-12 ml (but mostly 6-8  
410 ml), as opposed to the volume range of 8 up to 40 ml collected for the  $C_{HPLC}$  tests. In short,  
411 this volume range was too small for detection of a significant size dependence of  $C_{HPLC}$ . The

412 correct radiocarbon content ( $F_S$ ) values from the individual samples are listed in Table 3.  
413 There was no evidence for a significant difference in the  $F^{14}\text{C}$  values between the B5CAs and  
414 B6CAs. Hence, replicate analyses of B5CAs and B6CAs from the same process standard  
415 were taken as equal. The 5 replicates of the modern charcoal sample give a mean  $F^{14}\text{C}$  value  
416 of 1.142, with a standard deviation of 0.025, i.e. a precision of 2.2%. This value mirrors both  
417 the  $F^{14}\text{C}$  of the digest (ETH-49860.1.1) and the reference analysis of the bulk material (ETH-  
418 50458). The individual samples exhibited values with a slightly greater uncertainty that in  
419 turn depended on the sample size and lower counting statistics. The largest sample containing  
420 27  $\mu\text{g C}$  had a precision of 2.9% and the smallest (16  $\mu\text{g C}$ ) a precision of 4.5%. Likewise, the  
421  $F_S$  for the largest sample (ETH-49868.1.1) was also the one closest to the reference value. The  
422 same was true for the fossil charcoal standard being depleted in  $^{14}\text{C}$ , even if no size dependent  
423 increase in precision is given for these duplicate values. The average  $F_S$  from 5 individual  
424 measurements was  $0.001 \pm 0.032$ . Samples with  $< 15 \mu\text{g C}$  were not analyzed, as  
425 demonstrated by Birkholz et al. (2013) that samples designated for CSRA and  $< 10 \mu\text{g C}$  are  
426 usually affected by  $C_{ex}$  to such an extent that no reliable results can be obtained. However, the  
427 data here demonstrate that sample amounts of 25 to 35  $\mu\text{g C}$  are suitable for high precision  
428 analysis. Additional replicate analyses are still recommended so that possible outliers can be  
429 easily identified. In summary, the given uncertainty in an individual measurement is  
430 satisfactory for C turnover studies or C source apportion. For precise dating purposes a higher  
431 precision is usually required. Indeed, there is room for further minimization of  $C_{ex}$ , especially  
432 during the HPLC isolation procedure. Comparing the background level of organic C in the  
433 ultra-pure water used (i.e. in the aqueous HPLC solvent) with published references indicates  
434 that the system used for this study could be improved with better maintenance. Lang et al.  
435 (2012) reported that not more than 0.04  $\mu\text{g C/ml}$  were detected in the aquatic mobile phase. In  
436 contrast, a concentration of up to 0.3  $\mu\text{g C/ml}$  was measured for the eluents used here.

#### 437 **4. Conclusions**

438 We present a method to purify individual BPCAs as compound-specific biomarkers for BC,  
439 followed by the determination of  $\delta^{13}\text{C}$  and  $F^{14}\text{C}$ . The combination of two measurements on  
440 the same sample reduces the efforts specified by an isolation protocol for the particular  
441 analysis. Furthermore, knowing both the  $\delta^{13}\text{C}$  and  $F^{14}\text{C}$  values for a sample helps interpret the  
442 results with respect to the impact of contamination that might be difficult to detect, especially  
443 when they have a different  $\delta^{13}\text{C}$  value from the sample of interest. Another benefit is the  
444 possibility of monitoring the development of the general  $C_{ex}$  background in an easy and cost  
445 effective way. C content and its  $\delta^{13}\text{C}$  value should give enough information and help avoid

446 expensive radiocarbon analysis of contaminated samples. Finally the wet oxidation method  
447 avoids the problems encountered in the combustion of H<sub>3</sub>PO<sub>4</sub>-rich sample residues.

448 A constant addition of extraneous C to the isolated samples was identified. Nevertheless, a  
449 size dependent component  $C_{ex}$  cannot be excluded. This is especially true for much larger  
450 samples (> 50 µg C) that need to be isolated with a greater extent of injections (e.g. 100-150  
451 injections to yield ca. 100 µg BPCA C). Contamination of  $1.6 \pm 0.2$  µg C, with F<sup>14</sup>C  $0.90 \pm$   
452  $0.14$ , was calculated. We have shown that the precision of individual measurements of  
453 samples with > 15 µg C is adequate for studies aimed at determining C turnover or source  
454 apportioning in soils and sediments. In addition, our data show that there is potential for also  
455 applying the method for dating purposes. Samples isolated in replicates each containing > 25  
456 µg C should give values precise enough for an age determination of, for example, combustion  
457 residues on pottery or other samples with very fine charcoal that cannot be analyzed directly  
458 or BC that is mixed with other OM. Based on the experience from study, we recommend that  
459 process standards and blanks are determined regularly, as it is possible that C concentration in  
460 chemicals and/or solvent changes through time.

461 The method can also be applied to other marker compounds (e.g. B4CA or B3CA), although  
462 it might require minor tuning of the HPLC method to obtain a clean chromatographic  
463 separation of the target compounds. Additional improvements could include the use of a  
464 HPLC column with more capacity to reduce the number of injections required for isolation of  
465 sufficient material. This might lead to less  $C_{ex}$ , although the flow rate would need to be  
466 increased.

## 467 **5. Author contributions**

468 The study was proposed by M.G., M.P.W.S., M.W.I.S., R.H.S. and S.M.B.; M.G. and  
469 M.P.W.S. carried out the experiments and data analysis. D.B.W., S.Q.L. and R.H.S. provided  
470 technical expertise for method development. I.H. carried out AMS analysis with solid  
471 graphite targets.

## 472 **Acknowledgements**

473 We would like to thank two anonymous reviewers for their constructive comments. Funding  
474 support from Swiss National Science Foundation (SNF) project Nr 200021-119950 / 200020-  
475 13484 and Nr 200020-131922, and also University of Zurich Forschungskredit Nr 57061004  
476 Fellowship is gratefully acknowledged. We thank M. Hilf, C. McIntyre and L. Wacker for  
477 assistance with HPLC and AMS measurements. T. Eglinton generously donated funding for

478 the AMS measurements. We also thank P. Ascough and M. Bird for donating the  
479 archaeological charcoal.

480 Associate Editor – M.J. Simpson

## 481 **References**

482 Alloway, B.V., Pribadi, A., Westgate, J.A., Bird, M., Fifield, L.K., Hogg, A., Smith, I., 2004.  
483 Correspondence between glass-FT and <sup>14</sup>C ages of silicic pyroclastic flow deposits sourced  
484 from Maninjau caldera, west-central Sumatra. *Earth and Planetary Science Letters* 227, 121–  
485 133.

486 Ascough, P.L., Bird, M.I., Brock, F., Higham, T.F.G., Meredith, W., Snape, C.E., Vane, C.H.,  
487 2009. Hydropyrolysis as a new tool for radiocarbon pre-treatment and the quantification of  
488 black carbon. *Quaternary Geochronology* 4, 140–147.

489 Bird, M.I., Ayliffe, L.K., Fifield, L.K., Turney, C.S.M., Cresswell, R.G., Barows, T.T.,  
490 David, B., 1999. Radiocarbon dating of “old” charcoal using a wet oxidation, stepped-  
491 combustion procedure. *Radiocarbon* 41, 127–140.

492 Birkholz, A., Smittenberg, R.H., Hajdas, I., Wacker, L., Bernasconi, S.M., 2013. Isolation and  
493 compound specific radiocarbon dating of terrigenous branched glycerol dialkyl glycerol  
494 tetraethers (brGDGTs). *Organic Geochemistry* 60, 9-19.

495 Carcaillet, C., Almquist, H., Asnong, H., Bradshaw, R.H.W., Carrión, J.S., Gaillard, M.-J.,  
496 Gajewski, K., Haas, J.N., Haberle, S.G., Hadorn, P., Müller, S.D., Richard, P.J.H., Richoz, I.,  
497 Rösch, M., Sánchez Goñi, M.F.S., Von Stedingk, H., Stevenson, A.C., Talon, B., Tardy, C.,  
498 Tinner, W., Tryterud, E., Wick, L., Willis, K.J., 2002. Holocene biomass burning and global  
499 dynamics of the carbon cycle. *Chemosphere* 49, 845–863.

500 Dittmar, T., 2008. The molecular level determination of black carbon in marine dissolved  
501 organic matter. *Organic Geochemistry* 39, 396–407.

502 Eglinton, T.I., Aluwihare, L.I., Bauer, J.E., Druffel, E.R.M., McNichol, A.P., 1996. Gas  
503 chromatographic isolation of individual compounds from complex matrices for radiocarbon  
504 dating. *Analytical Chemistry* 68, 904–912.

505 Glaser, B., Balashov, E., Haumaier, L., Guggenberger, G., Zech, W., 2000. Black carbon in  
506 density fractions of anthropogenic soils of the Brazilian Amazon region. *Organic*  
507 *Geochemistry* 31, 669–678.

508 Glaser, B., Haumaier, L., Guggenberger, G., Zech, W., 1998. Black carbon in soils: the use of  
509 benzenecarboxylic acids as specific markers. *Organic Geochemistry* 29, 811–819.



510 Goldberg, E.D., 1985. Black Carbon in the Environment. Properties and Distribution. Wiley,  
511 Chichester, UK.

512 Hajdas, I., Bonani, G., Thut, H., Leone, G., Pfenninger, R., Maden, C., 2004. A report on  
513 sample preparation at the ETH/PSI AMS facility in Zurich. Nuclear Instruments & Methods  
514 in Physics Research Section B-Beam Interactions with Materials and Atoms 223-224, 267–  
515 271.

516 Hammes, K., Smernik, R.J., Skjemstad, J.O., Herzog, A., Vogt, U.F., Schmidt, M.W.I., 2006.  
517 Synthesis and characterisation of laboratory-charred grass straw (*Oryza sativa*) and chestnut  
518 wood (*Castanea sativa*) as reference materials for black carbon quantification. Organic  
519 Geochemistry 37, 1629–1633.

520 Hedges, J.I., Eglinton, G., Hatcher, P.G., Kirchman, D.L., Arnosti, C., Derenne, S., Evershed,  
521 R.P., Kögel-Knabner, I., de Leeuw, J.W., Littke, R., Michaelis, W., Rullkötter, J., 2000. The  
522 molecularly-uncharacterized component of nonliving organic matter in natural environments.  
523 Organic Geochemistry 31, 945–958.

524 Knicker, H., Hilscher, A., González-Vila, F.J., Almendros, G., 2008. A new conceptual model  
525 for the structural properties of char produced during vegetation fires. Organic Geochemistry  
526 39, 935–939.

527 Lang, S.Q., Bernasconi, S.M., Früh-Green, G.L., 2012. Stable isotope analysis of organic  
528 carbon in small ( $\mu\text{g C}$ ) samples and dissolved organic matter using a GasBench preparation  
529 device. Rapid Communications in Mass Spectrometry 26, 9–16.

530 Lang, S.Q., Früh-Green, G.L., Bernasconi, S.M., Wacker, L., 2013. Isotopic ( $\delta^{13}\text{C}$ ,  $\Delta^{14}\text{C}$ )  
531 analysis of organic acids in marine samples using wet chemical oxidation. Limnology and  
532 Oceanography: Methods 11, 161–175.

533 Masiello, C.A., 2004. New directions in black carbon organic geochemistry. Marine  
534 Chemistry 92, 201–213.

535 Pearson, A., McNichol, A.P., Schneider, R.J., von Reden, K.F., 1998. Microscale AMS  $^{14}\text{C}$   
536 measurement at NOSAMS. Radiocarbon 40, 61–75.

537 Preston, C.M., Schmidt, M.W.I., 2006. Black (pyrogenic) carbon: a synthesis of current  
538 knowledge and uncertainties with special consideration of boreal regions. Biogeosciences 3,  
539 397–420.

540 Reimer, P.J., Brown, T.A., Reimer, R.W., 2004. Discussion: Reporting and calibration of  
541 post-bomb  $^{14}\text{C}$  data. Radiocarbon 46, 1299–1304.

542 Ruff, M., Wacker, L., Gäggeler, H.W., Suter, M., Synal, H.A., Szidat, S., 2007. A gas ion  
543 source for radiocarbon measurements at 200 kV. *Radiocarbon* 49, 307–314.

544 Schmidt, M.W.I., Noack, A.G., 2000. Black carbon in soils and sediments: Analysis,  
545 distribution, implications, and current challenges. *Global Biogeochemical Cycles* 14, 777–  
546 793.

547 Schneider, M.P.W., Smittenberg, R.H., Dittmar, T., Schmidt, M.W.I., 2011. Comparison of  
548 gas with liquid chromatography for the determination of benzenepolycarboxylic acids as  
549 molecular tracers of black carbon. *Organic Geochemistry* 42, 275–282.

550 Shah, S.R., Pearson, A., 2007. Ultra-microscale (5–25 µg C) analysis of individual lipids by  
551 <sup>14</sup>C AMS: Assessment and correction for sample processing blanks. *Radiocarbon* 49, 69–82.

552 Skjemstad, J.O., Clarke, P., Taylor, J.A., Oades, J.M., McClure, S.G., 1996. The chemistry  
553 and nature of protected carbon in soil. *Australian Journal of Soil Research* 34, 251–271.

554 Skjemstad, J.O., Dalal, R.C., Janik, L.J., McGowan, J.A., 2001. Changes in chemical nature  
555 of soil organic carbon in Vertisols under wheat in south-eastern Queensland. *Australian*  
556 *Journal of Soil Research* 39, 343–359.

557 Skjemstad, J.O., Spouncer, L.R., Cowie, B., Swift, R.S., 2004. Calibration of the Rothamsted  
558 organic carbon turnover model (RothC ver. 26.3), using measurable soil organic carbon pools.  
559 *Australian Journal of Soil Research* 42, 79–88.

560 Stuiver, M., Polach, H.A., 1977. Discussion: Reporting of <sup>14</sup>C data. *Radiocarbon* 19, 355–  
561 363.

562 Synal, H.A., Stocker, M., Suter, M., 2007. MICADAS: A new compact radiocarbon AMS  
563 system. *Nuclear Instruments & Methods in Physics Research Section B: Beam Interactions*  
564 *with Materials and Atoms* 259, 7–13.

565 Tinner, W., Conedera, M., Ammann, B., Lotter, A.F., 2005. Fire ecology north and south of  
566 the Alps since the last ice age. *The Holocene* 15, 1214–1226.

567 Wacker, L., Christl, M., Synal, H.A., 2010. Bats: A new tool for AMS data reduction. *Nuclear*  
568 *Instruments Methods in Physics Research Section B: Beam Interactions with Materials and*  
569 *Atoms* 268, 976–979.

570 Wacker, L., Fahrni, S.M., Hajdas, I., Molnar, M., Synal, H.-A., Szidat, S., Zhang, Y.L., 2013.  
571 A versatile gas interface for routine radiocarbon analysis with a gas ion source. *Nuclear*  
572 *Instruments and Methods in Physics Research Section B: Beam Interactions with Materials*  
573 *and Atoms* 294, 315–319.

574 Wacker, L., Lippold, J., Molnár, M., Schulz, H., 2013. Towards radiocarbon dating of single  
575 foraminifera with a gas ion source. *Nuclear Instruments and Methods in Physics Research*  
576 *Section B: Beam Interactions with Materials and Atoms* 294, 307–310.

577 Wiedemeier, D.B., Hilf, M.D., Smittenberg, R.H., Haberle, S.G., Schmidt, M.W.I., 2013.  
578 Improved assessment of pyrogenic carbon quantity and quality in environmental samples by  
579 high-performance liquid chromatography. *Journal of Chromatography A* 1304, 246–250.

580 Yarnes, C., Santos, F., Singh, N., Abiven, S., Schmidt, M.W.I., Bird, J.A., 2011. Stable  
581 isotopic analysis of pyrogenic organic matter in soils by liquid chromatography-isotope-ratio  
582 mass spectrometry of benzene polycarboxylic acids. *Rapid Communications in Mass*  
583 *Spectrometry* 25, 3723–3731.

584 Zencak, Z., Reddy, C.M., Teuten, E.L., Xu, L., McNichol, A.P., Gustafsson, Ö., 2007.  
585 Evaluation of gas chromatographic isotope fractionation and process contamination by carbon  
586 in compound-specific radiocarbon analysis. *Analytical Chemistry* 79, 2042–2049.

587 Zimmerman, A.R., 2010. Abiotic and microbial oxidation of laboratory-produced black  
588 carbon (biochar). *Environmental Science & Technology* 44, 1295–1301.

589 Ziolkowski, L.A., Druffel, E.R.M., 2009a. Quantification of extraneous carbon during  
590 compound specific radiocarbon analysis of black carbon. *Analytical Chemistry* 81, 10156–  
591 10161.

592 Ziolkowski, L.A., Druffel, E.R.M., 2009b. The feasibility of isolation and detection of  
593 fullerenes and carbon nanotubes using the benzene polycarboxylic acid method. *Marine*  
594 *Pollution Bulletin* 59, 213–218.

595

595 **Figure captions**

596 **Fig. 1.** HPLC-DAD chromatogram from a 5  $\mu$ l injection of a BPCA extract of modern char  
597 for fraction collection (A), and HPLC-DAD chromatograms of aliquots of purified B6CA and  
598 B5CA fractions detected at 216 and 240nm (B). Time windows for single peak collection of  
599 B6CA (B6) and B5CA (B5) are highlighted in the gray boxes.

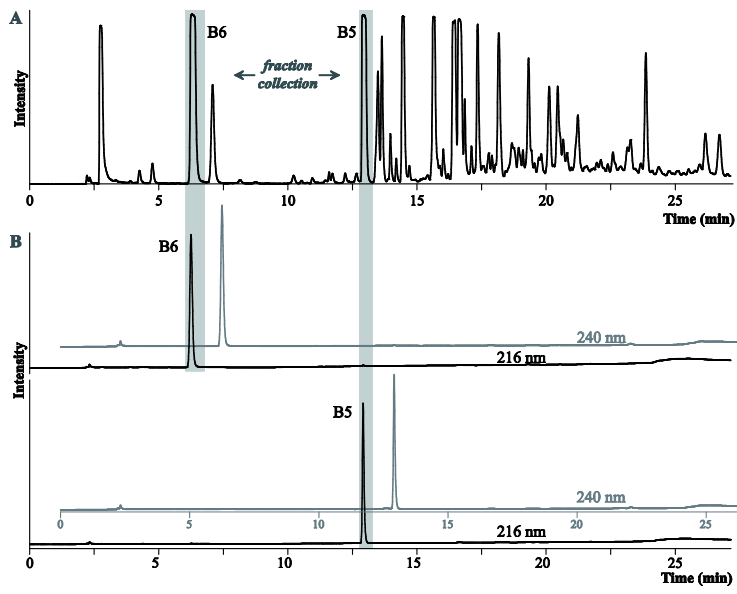
600 **Fig. 2.**  $\delta^{13}\text{C}$  values of individual B5CA and B6CA and of the whole BPCA digest of fossil  
601 (left) and modern char (right) measured in this study, and as published by Yarnes et al. (2011)  
602 for the modern char.

603 **Fig. 3.** Mass of HPLC blank vs. volume of collected eluent.

604 **Fig. 4.** Radiocarbon values for B5CA and B6CA isolated from the modern (left) and fossil  
605 char (right). The given error is composed of corrections for instrumental AMS background  
606 and the blank for wet oxidation. The solid gray line represents an idealized line for the  
607 mixture of the real  $\text{F}^{14}\text{C}$  value of sample and the determined mean external contamination.

608

608

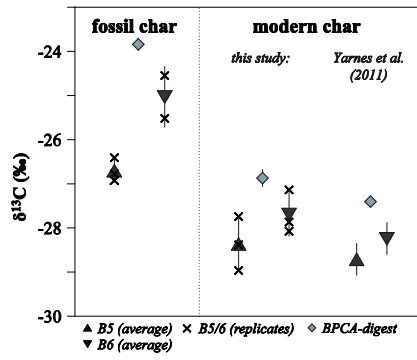


609

610 **Figure 1**

611

611

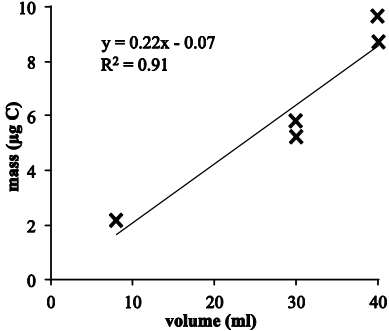


612

613 **Figure 2**

614

614

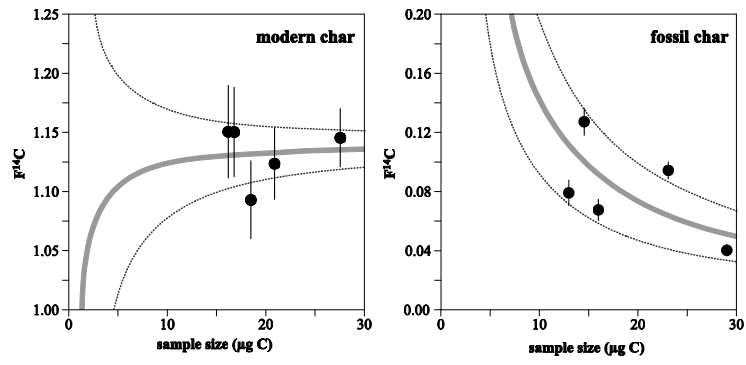


615

616 **Figure 3**

617

617



618

619 **Figure 4**

620

621

622

623



623 **Tables**624 **Table 1**625 Isolation of B5CA and B6CA from two process standards with HPLC, recovered mass as analyzed with HPLC  
626 and GC-IRMS and corresponding  $\delta^{13}\text{C}$  values.

Sample	Compound	HPLC			GC-IRMS		Yarnes et al., 2011
		Injection	$\mu\text{g C}^{\text{a}}$	Recovery	$\mu\text{g C}^{\text{b}}$	$\delta^{13}\text{C}$ (‰)	$\delta^{13}\text{C}$ (‰) <sup>c</sup>
Fossil char	Digest				43.4	$-23.8 \pm 0.1$	
	B6CA	20 $\times$ 5 $\mu\text{l}$	22.3	76%	29.3	$-25.5 \pm 0.3$	
	B6CA	30 $\times$ 5 $\mu\text{l}$	35.2	80%	39.7	$-24.5 \pm 0.1$	
	Avg. B6CA					$-25.0 \pm 0.7$	
	B5CA	20 $\times$ 5 $\mu\text{l}$	16.3	55%	17.2	$-26.9 \pm 0.3$	
	B5CA	25 $\times$ 5 $\mu\text{l}$	20.4	55%	21.7	$-26.4 \pm 0.3$	
	B5CA	30 $\times$ 5 $\mu\text{l}$	21.8	49%	22.9	$-26.8 \pm 0.2$	
	Avg. B5CA					$-26.7 \pm 0.4$	
Modern char	Digest				17.7	$-26.9 \pm 0.2$	$-27.4^{\text{d}}$
	B6CA	20 $\times$ 5 $\mu\text{l}$	19.9	74%	23.3	$-27.9 \pm 0.3$	
	B6CA	25 $\times$ 5 $\mu\text{l}$	28.6	84%	32.5	$-28.1 \pm 0.1$	
	B6CA	25 $\times$ 5 $\mu\text{l}$	25.9	76%	31.1	$-27.1 \pm 0.3$	
	Avg. B6CA					$-27.7 \pm 0.5$	$-28.24 \pm 0.36$
	B5CA	20 $\times$ 5 $\mu\text{l}$	19.7	50%	25.8	$-28.4 \pm 0.3$	
	B5CA	25 $\times$ 5 $\mu\text{l}$	30.6	62%	29.5	$-27.7 \pm 0.1$	
	B5CA	25 $\times$ 5 $\mu\text{l}$	25.3	52%	28.1	$-29.0 \pm 0.3$	
	Avg. B5CA					$-28.4 \pm 0.6$	$-28.71 \pm 0.36$

627 <sup>a</sup> Determined by comparing sample peak areas with those from a dilution series of BPCA standards with  
628 known concentration;629 <sup>b</sup> determined on amount of  $\text{CO}_2$  generated during oxidation in the headspace of the vials, by comparing peak  
630 areas with those of a series of standards of known concentration;631 <sup>c</sup> determined with ion chromatography IRMS;632 <sup>d</sup> bulk sample analyzed with EA-IRMS.633 **Table 2**634 Direct assessment of  $C_{\text{HPLC}}$  (n.a.: not analyzed).

Sample	HPLC	GC-IRMS		
	Collected ml	$\mu\text{g C}^{\text{a}}$	$\mu\text{g /ml}$	$\delta^{13}\text{C}$ (‰)
$C_{\text{chem.}+\text{HPLC}}$ <sup>b</sup>	20		$0.23 \pm 0.12$	n.a.
$C_{\text{HPLC}}$	40	9.7	0.24	$-28.6 \pm 0.1$
$C_{\text{HPLC}}$	40	8.7	0.22	$-28.5 \pm 0.1$
$C_{\text{HPLC}}$	8	2.2	0.28	n.a.
$C_{\text{HPLC}}$	30	5.2	0.17	$-29.8 \pm 0.1$
$C_{\text{HPLC}}$	30	5.8	0.19	$-31.4 \pm 0.1$
Avg. $C_{\text{HPLC}}$			$0.22 \pm 0.04$	$-29.5 \pm 1.3$

635 <sup>a</sup> Determined on amount of  $\text{CO}_2$  generated during oxidation in the headspace of the vials, by comparing peak  
636 areas with those of a series of standards of known concentration;637 <sup>b</sup> n = 2.

638

638  
639  
640

**Table 3**

Amount and radiocarbon content of isolated process standards B5CA and B6CA, calculated amount of external C ( $C_{ex}$ ) added to the related sample and residual  $F^{14}C$  values after correction for the blank ( $F_S$ ).

Sample		$F_T$ ( $F^{14}C$ ) <sup>a</sup>	$C_T$ ( $\mu g C$ )	Calculated $C_{ex}$ ( $\mu g C$ )	Corrected values $F_S$ ( $F^{14}C$ ) <sup>b</sup>	Lab code
Fossil char	Bulk <sup>c</sup>				0.003 ± 0.001	ETH-50456
	Digest				0.010 ± 0.002	ETH-49849
	B6CA	0.094 ± 0.004	23.1 ± 0.5	2.1 ± 0.1	0.036 ± 0.025	ETH-50461
	B6CA	0.040 ± 0.003	29.0 ± 0.5	1.1 ± 0.1	-0.009 ± 0.019	ETH-49854
	B5CA	0.079 ± 0.006	13.0 ± 0.5	1.0 ± 0.1	-0.033 ± 0.045	ETH-50459
	B5CA	0.068 ± 0.005	16.0 ± 0.5	1.0 ± 0.1	-0.022 ± 0.036	ETH-50460
	B5CA	0.127 ± 0.007	14.5 ± 0.5	1.8 ± 0.1	0.034 ± 0.040	ETH-49859
Modern extraneous C ( $F^{14}C = 1$ ) addition:				1.4 ± 0.5	Avg. $C_{ex}$	
Modern char	Bulk <sup>c</sup>				1.142 ± 0.004	ETH-50458
	Digest				1.143 ± 0.020	ETH-49860
	B6CA	1.151 ± 0.025	16.2 ± 0.5	-0.1 ± 0.5	1.162 ± 0.074	ETH-50462
	B6CA	1.093 ± 0.021	18.5 ± 0.5	0.8 ± 0.5	1.102 ± 0.056	ETH-49864
	B6CA	1.124 ± 0.020	20.9 ± 0.5	0.3 ± 0.5	1.132 ± 0.056	ETH-50463
	B5CA	1.145 ± 0.019	27.6 ± 0.5	-0.1 ± 0.6	1.152 ± 0.034	ETH-49868
	B5CA	1.150 ± 0.024	16.8 ± 0.5	-0.1 ± 0.5	1.161 ± 0.071	ETH-50465
Radiocarbon dead extraneous C ( $F^{14}C = 1$ ) addition:				0.2 ± 0.4	Avg. $C_{ex}$	

641  
642  
643  
644  
645  
646  
647

- <sup>a</sup> Subscript  $T$  indicates that values were corrected for instrumental background using the BATS program (Wacker, 2010) and for the wet oxidation procedure (Lang et al., 2013);
- <sup>b</sup> subscript  $S$  indicated that values were corrected for mean modern or radiocarbon dead extraneous carbon addition occurring during the entire laboratory protocol. Please note that the fractions of 'bulk' and 'extract' required less corrections than those isolated by HPLC.
- <sup>c</sup>  $^{14}C$  values from bulk sample material were corrected for instrumental background using BATS software.

647 **Supplementary**

648 **A. Correction for wet oxidation procedure**

649 **A. Tables**

650 **Table A 1:** Amounts and radiocarbon contents of the isolated process standards of the wet oxidation – phthalic  
 651 acid and sucrose with the corresponding calculated amount of external C ( $C_{ex}$ ) added to the standard, and the  
 652 residual  $F^{14}C$  values after correction for the blank ( $F_S$ ).

Standard	BATS output		Calculated $C_{ex}$ ( $\mu\text{g C}$ )	Corrected values $F_S$ ( $F^{14}C$ )	Lab code
	$F_T$ ( $F^{14}C$ ) <sup>a</sup>	$C_T$ ( $\mu\text{g C}$ )			
<i>1<sup>st</sup> campaign</i>					
Phthalic acid <sup>b</sup>	0.0140 ± 0.002	12.4 ± 0.5	0.14 ± 0.03	0.004 ± 0.004	ETH-49846.11.1
	0.0165 ± 0.003	13.4 ± 0.5	0.19 ± 0.04	0.007 ± 0.004	ETH-49846.12.1
	0.0078 ± 0.002	15.3 ± 0.5	0.08 ± 0.03	-0.001 ± 0.003	ETH-49846.17.1
	0.0083 ± 0.002	17.8 ± 0.5	0.10 ± 0.04	0.001 ± 0.003	ETH-49846.7.1
	0.0084 ± 0.002	21.0 ± 0.5	0.12 ± 0.03	0.002 ± 0.003	ETH-49846.13.1
<i>Average addition of <math>C_{ex}</math> with <math>F^{14}C = 1</math>:</i>			<b>0.13 ± 0.04</b>		
Sucrose <sup>c</sup>	1.018 ± 0.012	17.4 ± 0.5	0.58 ± 0.88	1.070 ± 0.050	ETH-49845.2.1
	1.004 ± 0.011	21.5 ± 0.5	1.01 ± 0.95	1.045 ± 0.040	ETH-49845.1.1
	1.012 ± 0.012	21.7 ± 0.5	0.85 ± 0.96	1.053 ± 0.040	ETH-49845.3.1
	1.004 ± 0.012	23.4 ± 0.5	1.09 ± 1.00	1.042 ± 0.037	ETH-49845.4.1
	1.026 ± 0.012	27.3 ± 0.5	0.70 ± 1.09	1.059 ± 0.033	ETH-49845.12.1
<i>Average addition of <math>C_{ex}</math> with <math>F^{14}C = 0</math>:</i>			<b>0.85 ± 0.44</b>		
<i>2<sup>nd</sup> campaign</i>					
Phthalic acid	0.0243 ± 0.007	3.7 ± 0.5	0.08 ± 0.03	0.005 ± 0.012	ETH-49846.23.1
	0.0049 ± 0.003	9.1 ± 0.5	0.02 ± 0.03	-0.003 ± 0.005	ETH-49846.31.1
	0.0080 ± 0.003	11.5 ± 0.5	0.06 ± 0.04	0.002 ± 0.004	ETH-49846.25.1
	0.0086 ± 0.003	13.8 ± 0.5	0.08 ± 0.04	0.003 ± 0.004	ETH-49846.26.1
	0.0080 ± 0.003	20.0 ± 0.5	0.11 ± 0.07	0.004 ± 0.004	ETH-49846.30.1
<i>Average addition of <math>C_{ex}</math> with <math>F^{14}C = 1</math>:</i>			<b>0.07 ± 0.03</b>		
Sucrose	1.0016 ± 0.012	11.6 ± 0.5	0.57 ± 0.78	1.042 ± 0.066	ETH-49845.17.1
	1.0161 ± 0.013	12.4 ± 0.5	0.43 ± 0.79	1.054 ± 0.063	ETH-49845.18.1
	1.0359 ± 0.011	17.9 ± 0.5	0.29 ± 0.89	1.062 ± 0.044	ETH-49845.22.1
	1.0315 ± 0.010	24.0 ± 0.5	0.49 ± 1.00	1.051 ± 0.033	ETH-49845.20.1
<i>Average addition of <math>C_{ex}</math> with <math>F^{14}C = 0</math>:</i>			<b>0.45 ± 0.43</b>		

653 <sup>a</sup> Subscript  $T$  indicates that values have been corrected for instrumental background using the program BATS  
 654 (Wacker, 2010) and for the wet oxidation procedure (Lang et al., 2013), if required.

655 <sup>b</sup> The radiocarbon content of  $1.053 \pm 0.03 F^{14}C$  was determined on the powdered phthalic acid standard by  
 656 conventional AMS methods.

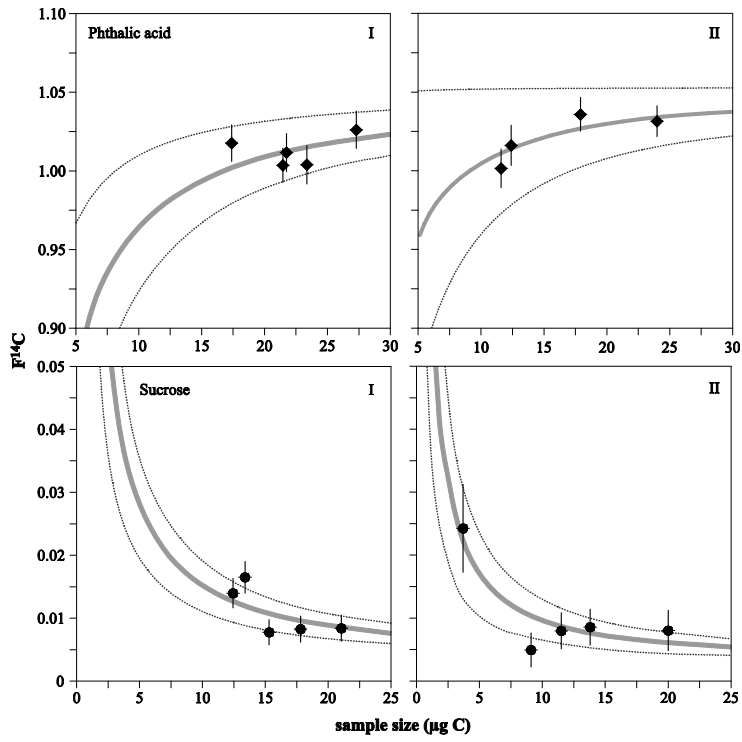
657 <sup>c</sup> The radiocarbon content of  $\leq 0.0025 F^{14}C$  was determined on the powdered sucrose standard by  
 658 conventional AMS methods.

659 **A. Figure caption**

660 **Figure A 1:** Radiocarbon values of phthalic acid (above) and sucrose (below) after the wet oxidation procedure of  
 661 both campaigns (I left, and II right). The given error bars derive only from corrections of instrumental AMS  
 662 background and counting statistics. The solid grey line represents an idealized line of the mixture of the  $F^{14}C$  value  
 663 of the process standard and the mean external contamination of modern ( $F^{14}C = 1$ , Phthalic acid) or radiocarbon  
 664 dead ( $F^{14}C = 0$ , Sucrose) carbon.

665

665



666

667 **Figure A1**

668

669

669  
670

671 **B. Direct assessment of  $C_{chemistry}/C_{HPLC}$**

672 **B. Table**

673 **Table B 1:** Amounts and radiocarbon contents of isolated process standards B5CA and B6CA, the volume of  
674 collected eluent of each sample and the calculated amount of external C ( $C_{ex}$ ) and its radiocarbon content ( $F_{ex}$ ),  
675 assuming that a  $C_{ex}$  of  $0.22 \pm 0.04 \mu\text{g ml}^{-1}$  elutes with the mobile phase.

Sample	$F_T$ ( $F^{14}\text{C}$ ) <sup>a</sup>	$C_T$ ( $\mu\text{g C}$ )	Collected $V_{el}$ (ml)	Calculated		Lab code	
				$C_{ex}$ ( $\mu\text{g C}$ )	$F_{ex}$ ( $F^{14}\text{C}$ )		
<b>Fossil char</b>	B6CA	$0.094 \pm 0.004$	$23.1 \pm 0.2$	4	0.9	2.4	ETH-50461.1.1
	B6CA	$0.040 \pm 0.003$	$29.0 \pm 0.3$	9	2.0	0.5	ETH-49854.1.1
	B5CA	$0.079 \pm 0.006$	$13.0 \pm 0.2$	4	0.9	1.1	ETH-50459.1.1
	B5CA	$0.068 \pm 0.005$	$16.0 \pm 0.2$	5	1.1	0.9	ETH-50460.1.1
	B5CA	$0.127 \pm 0.007$	$14.5 \pm 0.3$	12	2.6	0.7	ETH-49859.1.1
				<b>Average <math>F_{ex}</math></b>		<b>1.1</b>	
<b>Modern char</b>	B6CA	$1.151 \pm 0.025$	$16.2 \pm 0.2$	6	1.3	1.2	ETH-50462.1.1
	B6CA	$1.093 \pm 0.021$	$18.5 \pm 0.2$	8	1.8	1.6	ETH-49864.1.1
	B6CA	$1.124 \pm 0.020$	$20.9 \pm 0.2$	8	1.8	0.8	ETH-50463.1.1
	B5CA	$1.183 \pm 0.023$	$22.0 \pm 0.3$	5	1.1	0.2	ETH-50464.1.1
	B5CA	$1.145 \pm 0.019$	$27.6 \pm 0.3$	5	1.1	1.1	ETH-49868.1.1
	B5CA	$1.150 \pm 0.024$	$16.8 \pm 0.2$	6	1.3	1.2	ETH-50465.1.1
				<b>Average <math>F_{ex}</math></b>		<b>1.0</b>	

676 <sup>a</sup> Subscript *T* indicates that values have been corrected for instrumental background using the program BATS  
677 (Wacker, 2010) and for the wet oxidation procedure (Lang et al., 2013).